High-Q^2 Charged and Neutral Current Cross Sections With Polarised Positron Beam At ZEUS

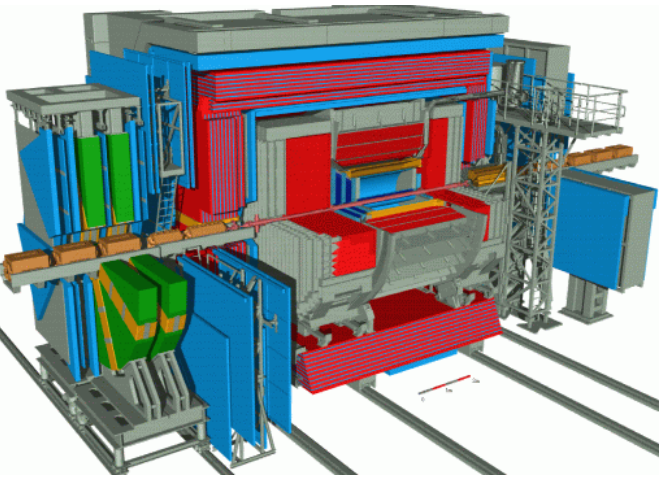

Trevor Stewart
University of Toronto

On Behalf of the ZEUS Collaboration

EPS 2011, 21-27 July,
Grenoble, France

1. **Charged current e^+p.**
2. **Neutral current e^+p.**
   - **High-x**

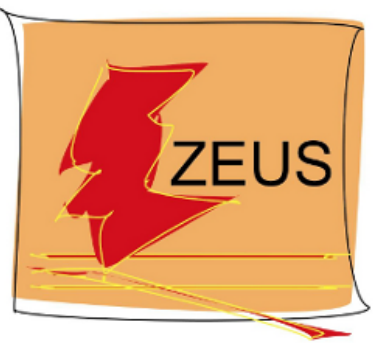

UNIVERSITY OF TORONTO

HERA II with Longitudinal Polarised $e^{\pm}$ Beams

- $e^{\pm}p$ collider with centre-of-mass energy: 318 GeV
- Two general purpose experiments, H1 and ZEUS (ZEUS data to be shown).
- $\approx 0.5 fb^{-1}$ taken by each experiment.

- HERA II upgrade: Longitudinally polarised $e^{\pm}$ beams.
  Mean longitudinal polarisation, $P_e = (N_R - N_L)/(N_R + N_L) \approx 30 - 40\%$

Deep Inelastic Scattering

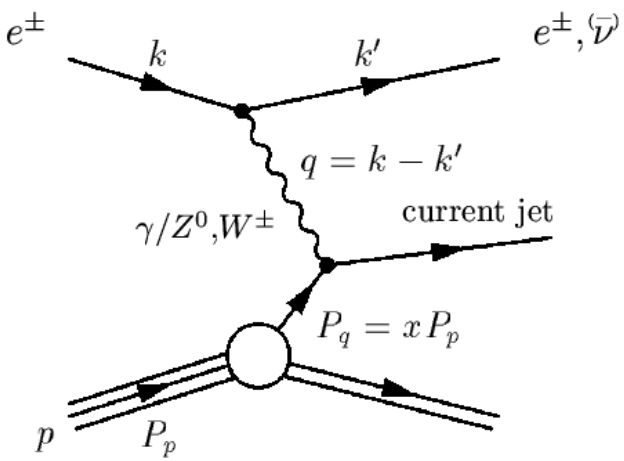

- Neutral Current (NC), γ or Z_0 exchange.
  $e^{\pm}p \rightarrow e^{\pm}X$
- Charged Current (CC), $W^{\pm}$ exchange.
  $e^{\pm}p \rightarrow \nu X$

Variables which characterize DIS:

- Q^2 probing power, negative 4-momentum squared:
  $Q^2 = -q^2 = -(k - k^{'})$
- Bjorken x, momentum fraction of proton carried by struck quark:
  $x = Q^2/2p \cdot q$
- Inelasticity y:
  $y = p \cdot q/p \cdot k$
- s is the centre-of-mass energy squared:
  $s = (p + k)^2$
- These are related by:
  $Q^2 = sxy$

Charged and Neutral Current events in the ZEUS detector

Charged Current

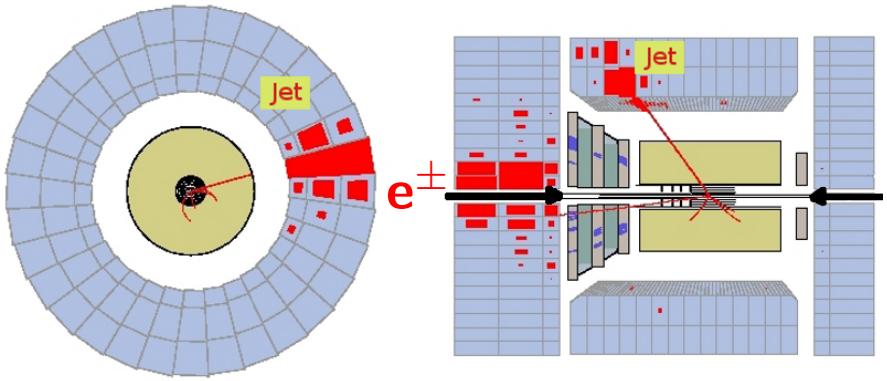

- $\nu(\bar{\nu})$ escapes the detector volume.
- Jet energy deposits not balanced by $e^{\pm}$ deposits.
- Characterised by missing-P_t.
- Kinematics reconstructed from hadrons.

Neutral Current

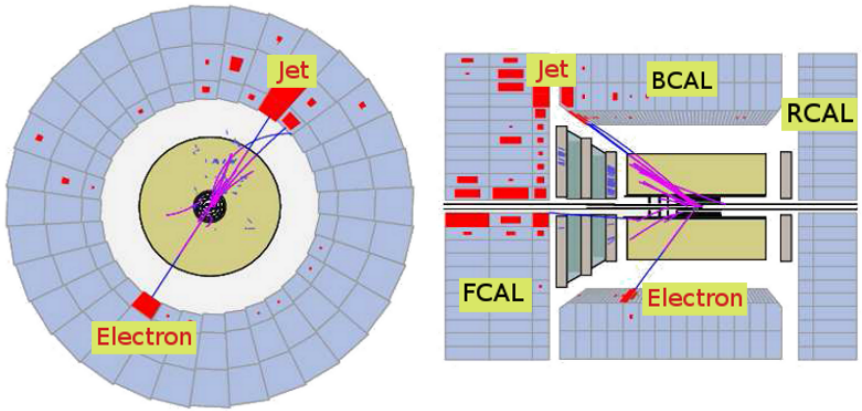

- Well measured scattered $e^{\pm}$.
- $e^{\pm}$ energy deposits and Jet(s) balanced in ϕ.
- Kinematics may be reconstructed in multiple ways.

Motivation: PDFs

Why are High Precision High-Q^2 CC and NC measurements important?

- The CC cross sections give a powerful probe of the flavour specific parton distributions (PDFs).
- The NC cross sections are sensitive to all flavours.

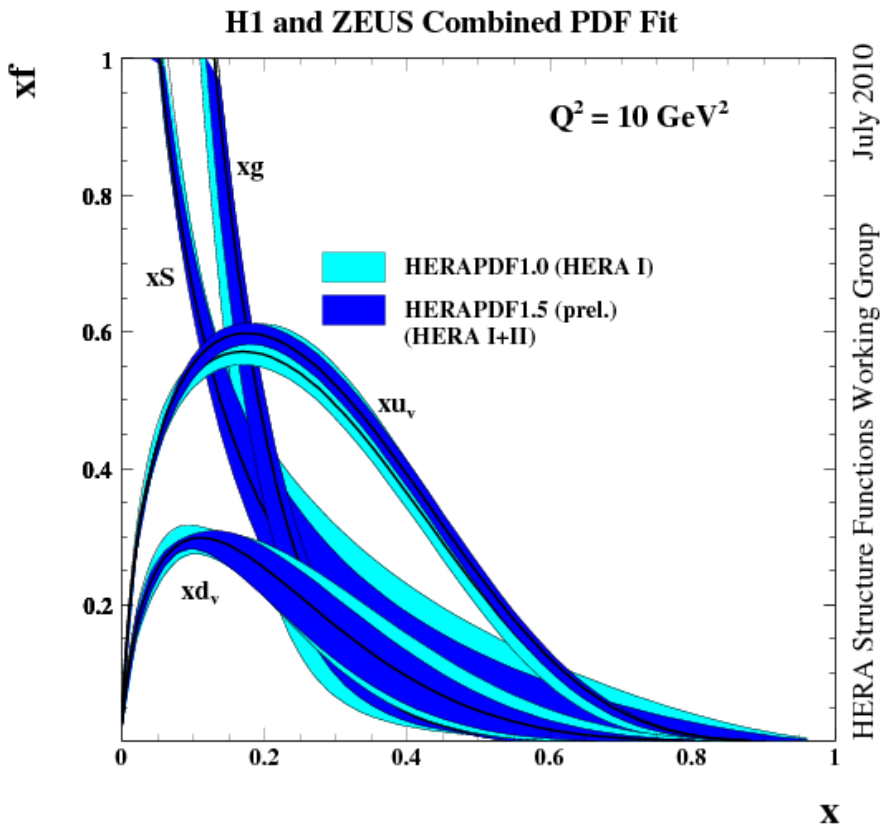

Motivation: Electroweak

Why are High Precision High-Q^2 CC and NC measurements important?

- Provides an excellent environment to test electroweak (EW) theory.
- The difference between the e^+p and e^-p NC cross sections give direct access to the structure function xF_3.
- The longitudinal polarisation asymmetry, $A^+ \approx a_e v_q$ allows parity violation to be directly measured.

Charged Current Cross Section

In the SM the $W^{\pm}$ interact only with left(right) (anti-)particles.

$$\sigma_{CC}^{e^{\pm}p} = (1 \pm P_e)\sigma_{CC,P_e=0}^{e^{\pm}p}$$

$$\frac{d^2\sigma_{CC}^{e^{\pm}p}}{dxdQ^2} = (1 \pm P_e)\frac{G_F^2}{4\pi x}\left(\frac{M_W^2}{M_W^2 + Q^2}\right)^2 \tilde{\sigma}_{CC}^{e^{\pm}p}$$

where $\tilde{\sigma}_{CC}^{e^{\pm}p}$ is the reduced cross section. e^+ and e^- sensitive to different quark densities, given at LO by:

$$\tilde{\sigma}_{CC}^{e^+p} = x[(\bar{u} + \bar{c}) + (1-y)^2(d+s)]$$

$$\tilde{\sigma}_{CC}^{e^-p} = x[(u + c) + (1-y)^2(\bar{d} + \bar{s})]$$

Total cross section with positive and negative P_e

Results published in 2010.
Eur. Phys. J. C (2010) 70: 945963.

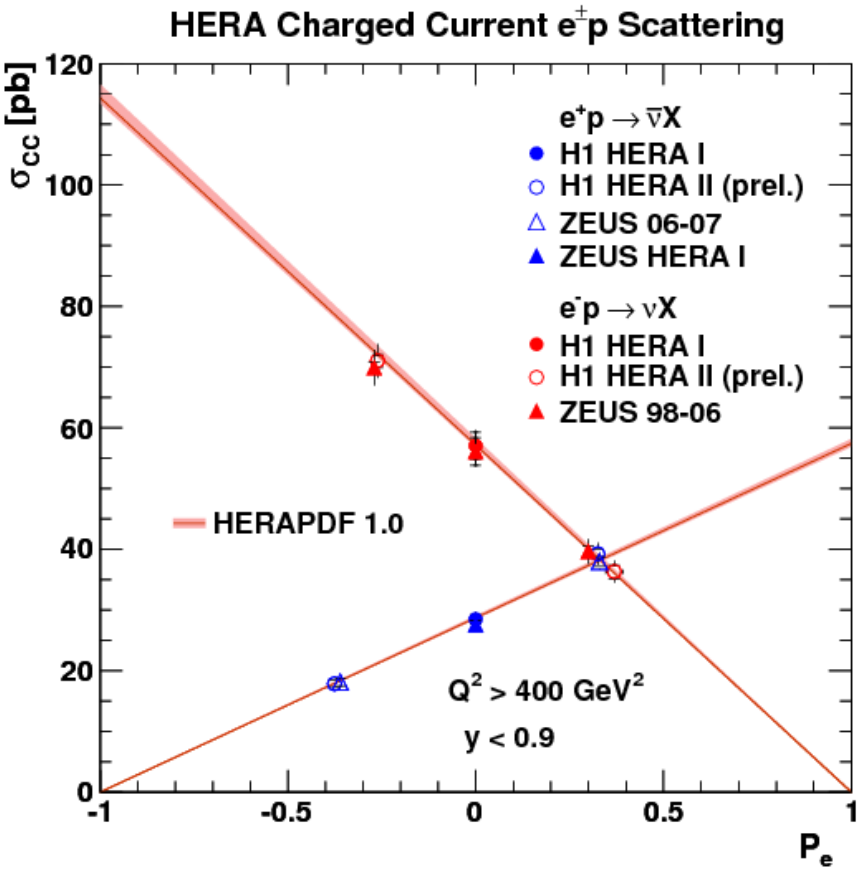

- The total cross section as a function of the longitudinal polarisation of the lepton beam.
  - Previous e^+p and e^-p results from H1 and ZEUS also shown.
  - Excellent test of EW theory.
- Results not included in SM predictions (HERAPDF1.0).
  - SM describes data well.

Total cross section at multiple polarisation values

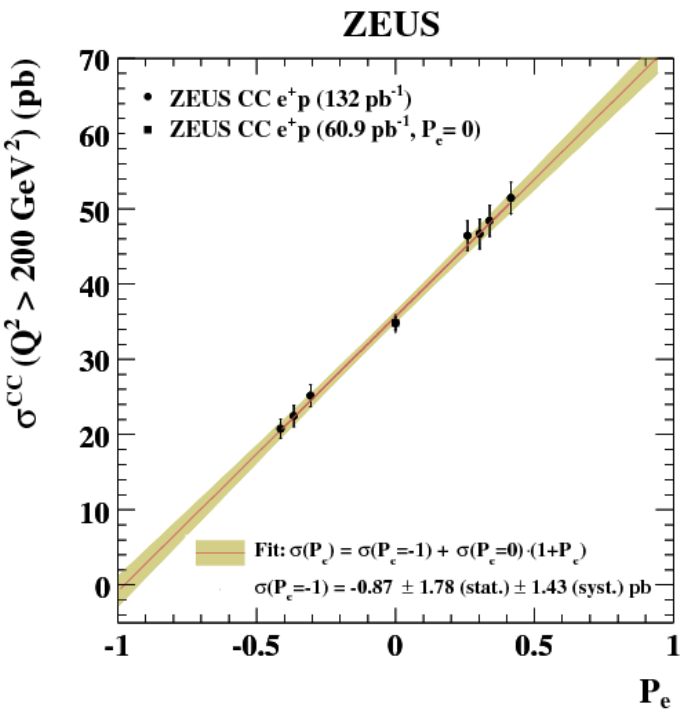

- CC e^+p Cross section becomes 0 for $P_e = -1$ positron beam.
  - A non-zero cross section might point to the existence of a right-handed W boson, W_R.
- Extrapolation to P_e=-1 consistent with 0.
- Limit placed on $\sigma^{CC}(P_e = -1)$ and M_{W_R} GeV consistent with other experiments.
  - $M_{W_R} > 198$GeV at 95% CL

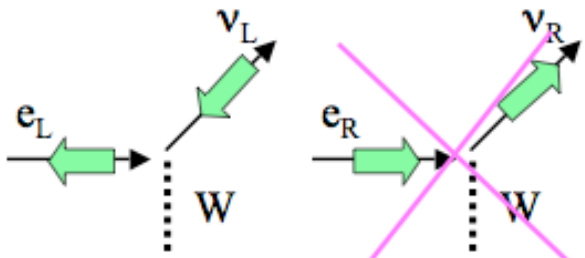

$d\sigma/dQ^2$ with positive and negative P_e

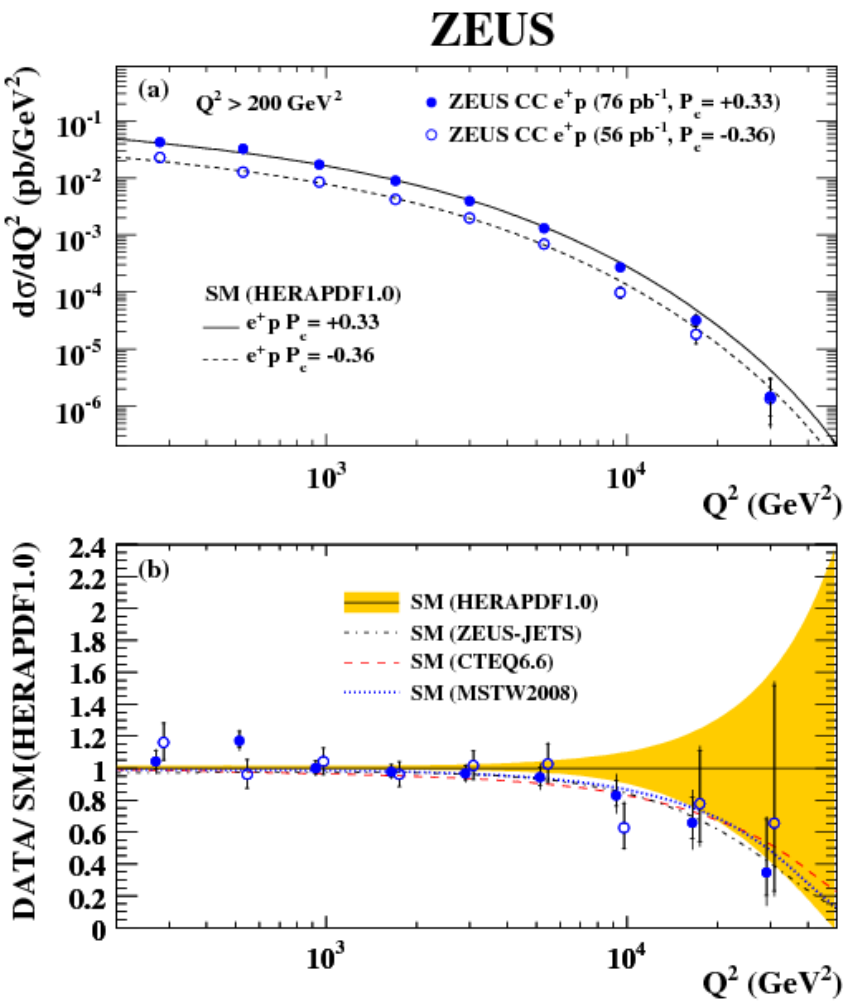

- Overall shift in cross sections due to effect of polarisation.
- Test of EW theory
- SM expectation in good agreement with data.

$d\sigma/dx$ and $d\sigma/dy$ with positive and negative P_e

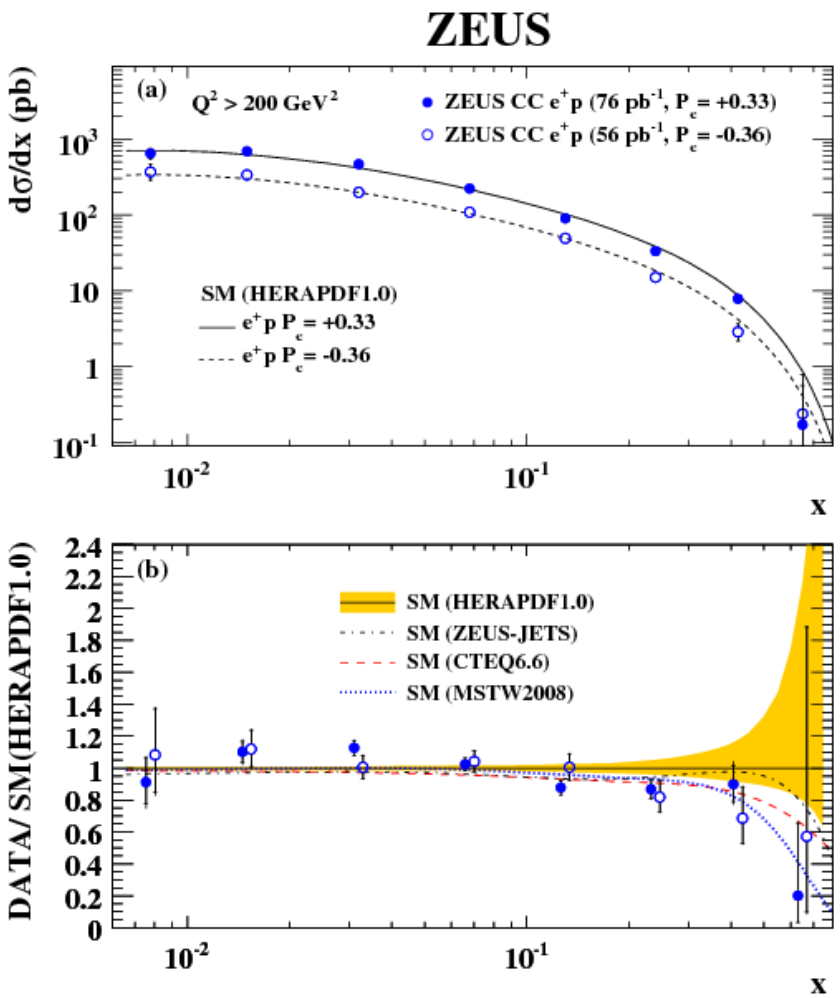

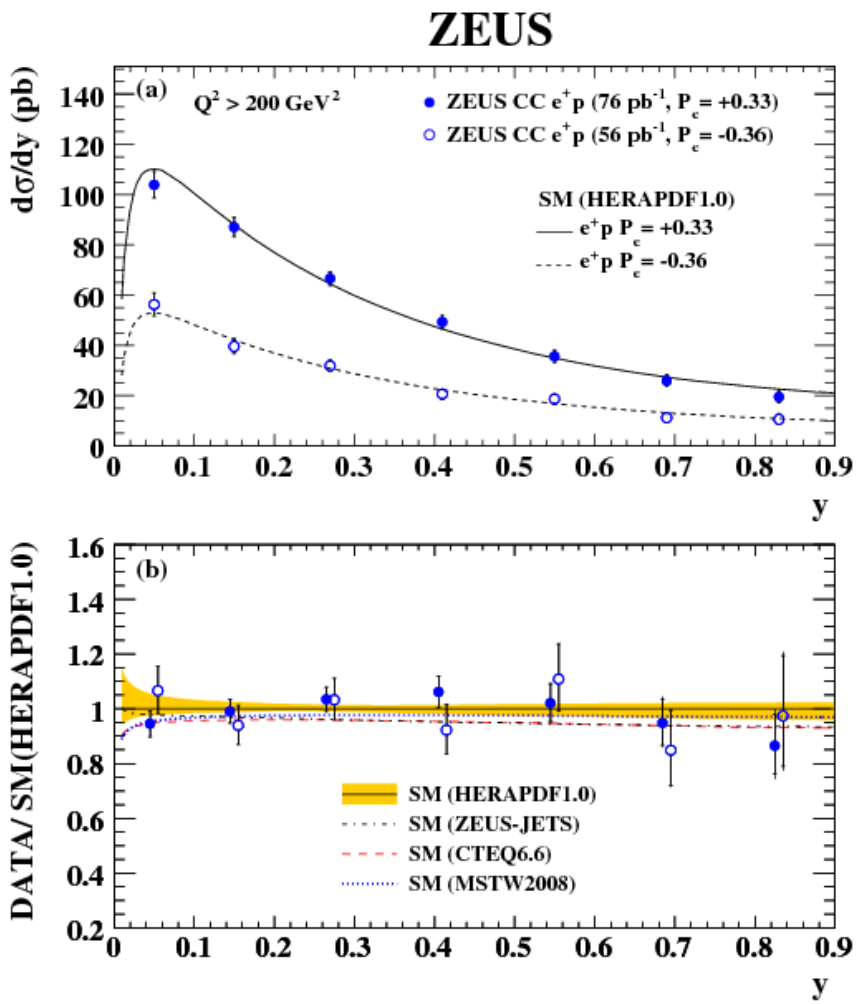

$\tilde{\sigma}$ with positive and negative P_e

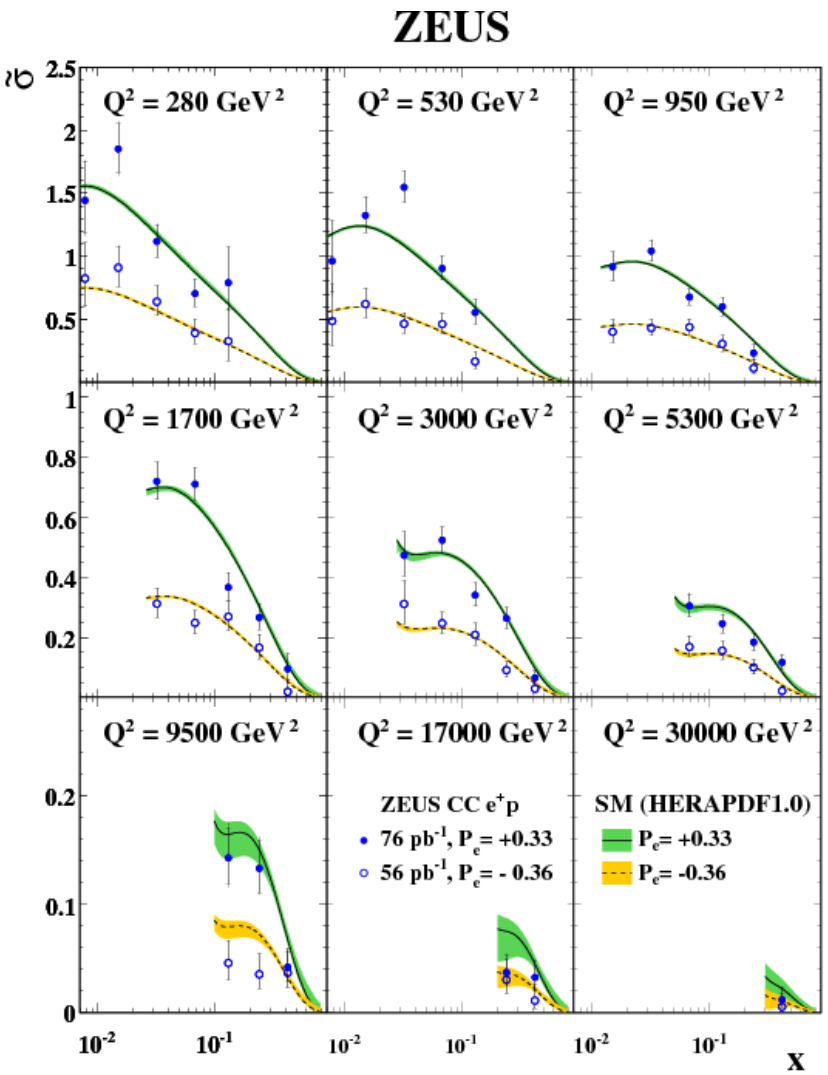

- Effect of polarisation clearly seen.
- SM predictions in good agreement with data.
  - Polarised data well understood. Results can be used to extract PDFs.

$\tilde{\sigma}$ with $P_e = 0$ (1)

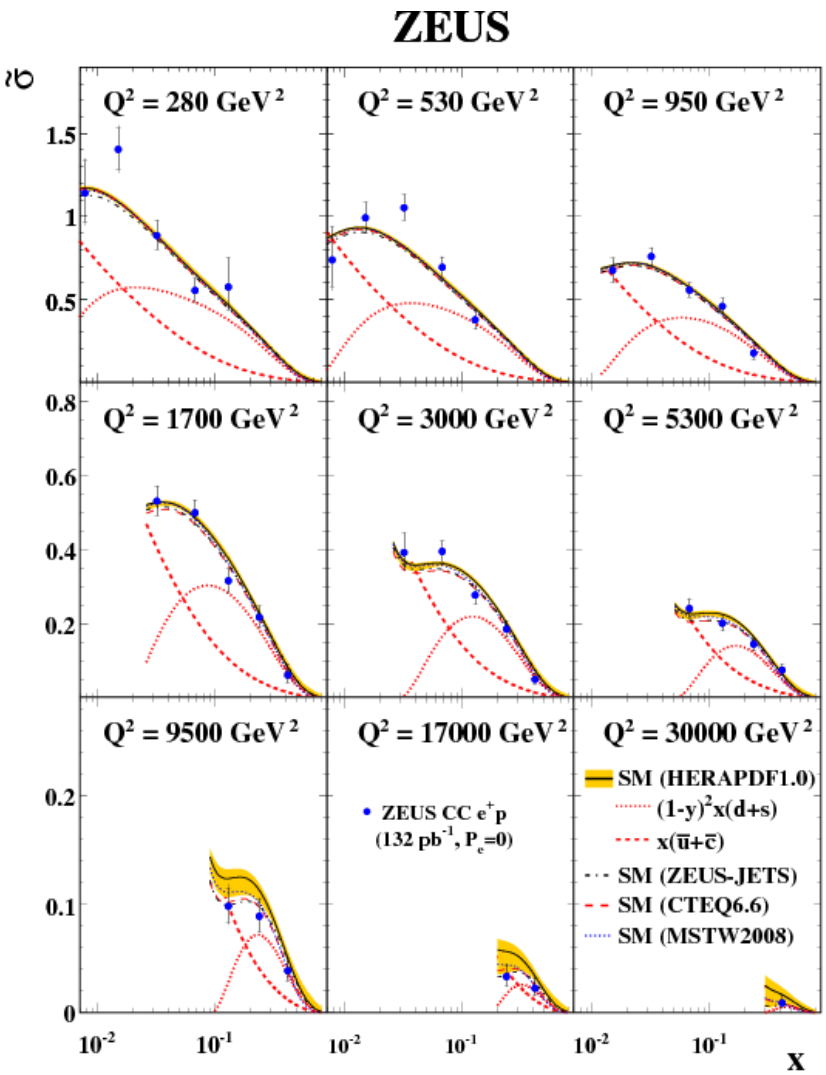

- The e^+p CC reduced cross section constrains the d quark density.
- As seen earlier, the reduced cross section, $\tilde{\sigma}$, at LO can be written as a sum of $x(\bar{u}+\bar{c})$ and $(d+s)$ contributions.

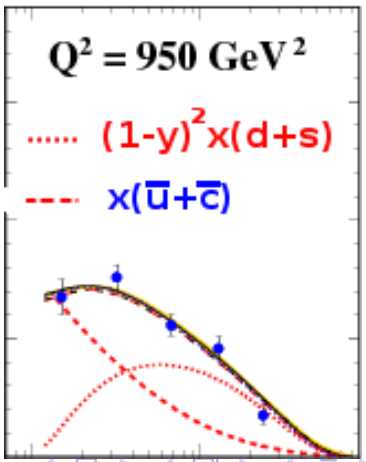

$\tilde{\sigma}$ with $P_e = 0$ (2)

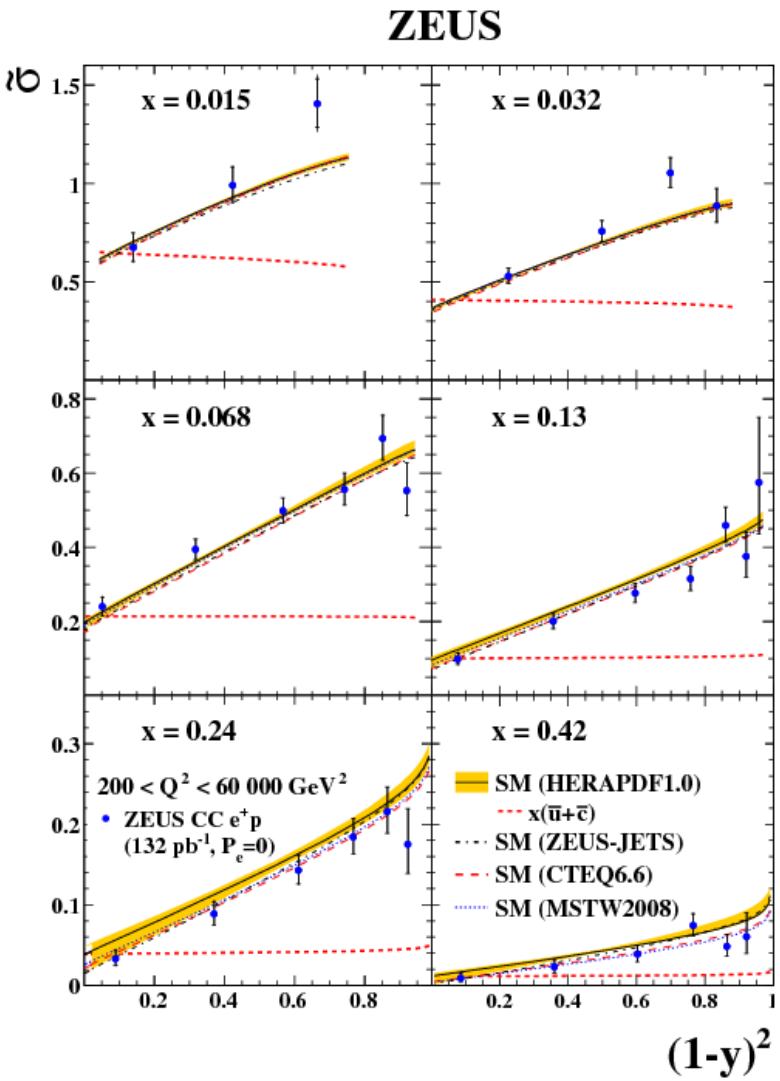

- SM W boson couples only to left(right)-handed (anti-)fermions.
  - $e^+\bar{q}$ distribution will be flat.
  - e^+q will exhibit a $(1-y)^2 \propto (1+cos\theta^*)^2$ distribution.
- $\tilde{\sigma}^{e^+p}_{CC} = x[(\bar{u}+\bar{c})+(1-y)^2(d+s)]$
  - At LO the intercept gives the $(\bar{u}+\bar{c})$ contribution.
  - $(d+s)$ is given by the slope.

Neutral Current Cross Section

- Mediated by both γ and Z_0

$$\frac{d^2\sigma_{NC}^{e^+p}}{dxdQ^2} = \frac{2\pi\alpha^2}{xQ^4}[Y_+\tilde{F}_2 \mp Y_- x\tilde{F}_3 - y^2\tilde{F}_L]$$

$$\tilde{\sigma}_{NC}^{e^\pm p} = \frac{xQ^4}{2\pi\alpha^2}\frac{1}{Y_+}\frac{d^2\sigma_{NC}^{e^+p}}{dxdQ^2} = \tilde{F}_2 \mp \frac{Y_-}{Y_+}x\tilde{F}_3 - \frac{y^2}{Y_+}\tilde{F}_L$$

- Where $\tilde{F}_2$,$x\tilde{F}_3$ and $\tilde{F}_L$ are the generalised structure functions.
- $Y_\pm$ is given by:

$$Y_\pm = 1 \pm (1-y)^2$$

Generalised Structure Functions

- The generalized structure functions are given by:

$$\tilde{F}_2 = F_2^{\gamma} + \kappa(-\nu_e \pm P_e a_e)F_2^{\gamma Z} + \kappa^2(\nu_e^2 + a_e^2 \pm 2P_e\nu_e a_e)F_2^{Z}$$

$$x\tilde{F}_3 = \kappa(-a_e \mp P_e\nu_e)xF_3^{\gamma Z} + \kappa^2(2\nu_e a_e \pm P_e(\nu_e^2 + a_e^2))xF_3^{Z}$$

$$\text{where } \kappa = \frac{1}{sin^2 2\theta_w}\frac{Q^2}{Q^2 + M_Z^2}$$

$$\{F_2^{\gamma}, F_2^{\gamma Z}, F_2^{Z}\} = \sum_q \{e_q^2, 2e_q\nu_q, v_q^2 + a_q^2\}x(q + \bar{q})$$

$$\{xF_3^{\gamma Z}, xF_3^{Z}\} = \sum_q \{e_q a_q, v_q a_q\}2x(q - \bar{q})$$

- $\tilde{F}_2$ dominates $\tilde{\sigma}_{NC}^{e^{\pm}p}$.
- $x\tilde{F}_3$ contributes only at high Q^2.
- $\tilde{F}_L$ contributes at high y (see previous slide).

$d\sigma/dQ^2$ with positive and negative P_e

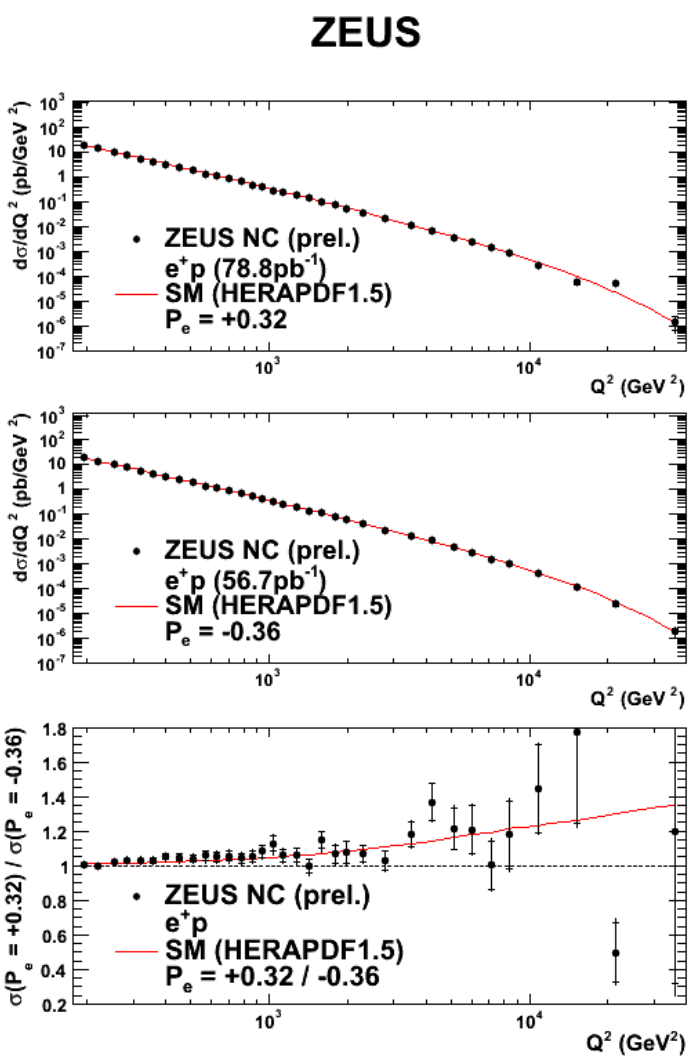

- The difference between the two polarisation states clearly seen at higher-Q^2.

← RH: $d\sigma/dQ^2$ with positive P_e.

← LH: $d\sigma/dQ^2$ with negative P_e.

← RH/LH: ratio of cross sections positive P_e/negative P_e.

- These results not included in the shown SM expectation (HERAPDF1.5).

Asymmetry

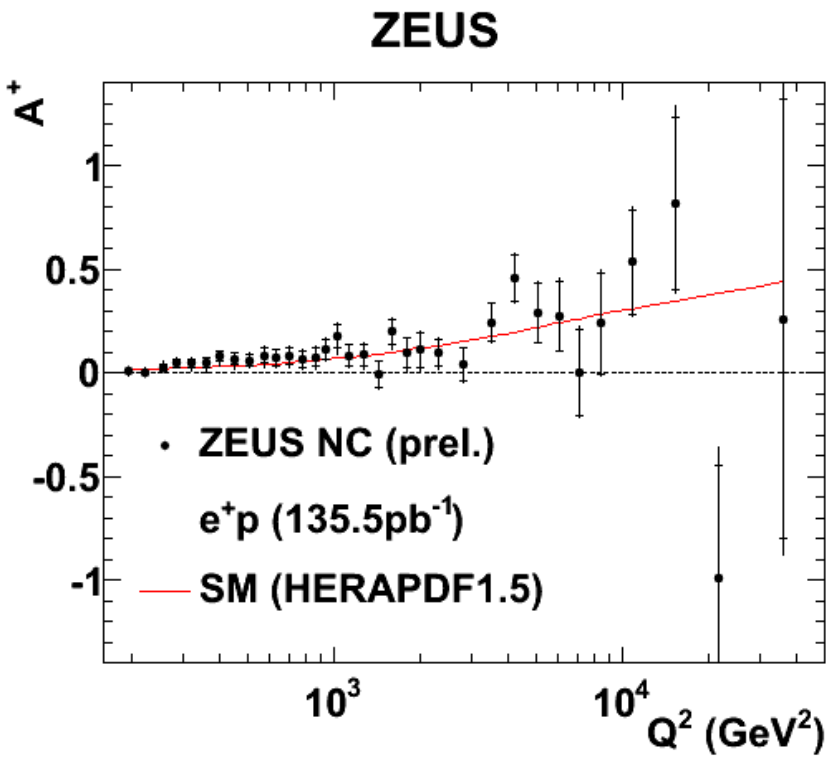

$$A^+ = \frac{2}{P_+ - P_-}\frac{\sigma^+(P_+) - \sigma^+(P_-)}{\sigma^+(P_+) + \sigma^+(P_-)}$$

- $A^+ \approx a_e \kappa \frac{F_2^{\gamma Z}}{F_2^{\gamma}} = a_e \kappa \frac{2 e_q \nu_q}{e_q^2} \propto a_e \nu_q$
- A^+ sensitive to ν_q.
- A^+ increase with Q^2.

$$\tilde{F}_2 = F_2^{\gamma} + \kappa(-\nu_e \pm P_e a_e)F_2^{\gamma Z} + \kappa^2(\nu_e^2 + a_e^2 \pm 2P_e \nu_e a_e)F_2^{Z}$$

$$x\tilde{F}_3 = \kappa(-a_e \mp P_e \nu_e)xF_3^{\gamma Z} + \kappa^2(2\nu_e a_e \pm P_e(\nu_e^2 + a_e^2))xF_3^{Z}$$

$d\sigma/dx$ and $d\sigma/dy$ with positive and negative P_e

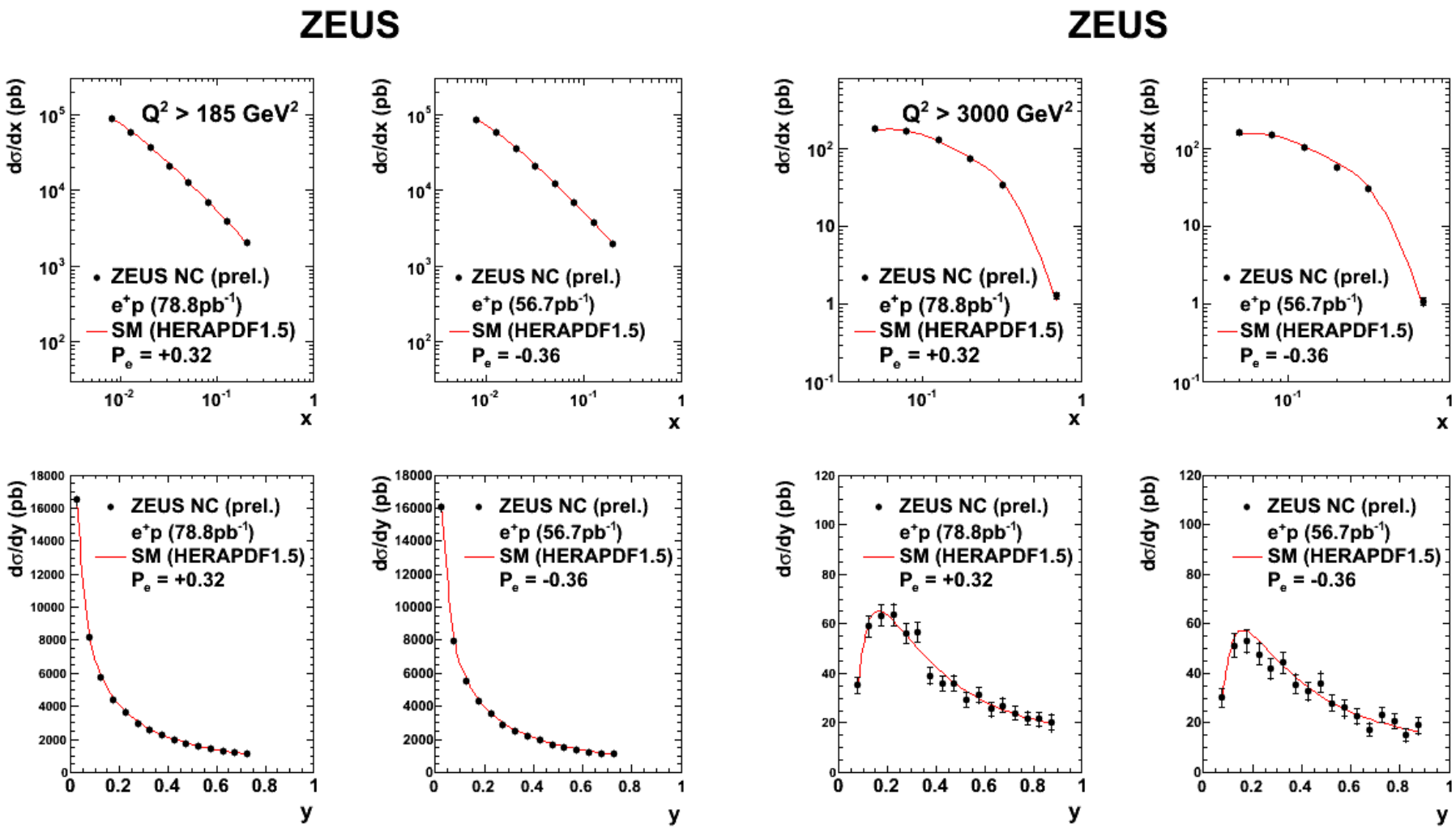

$\tilde{\sigma}$ with positive and negative P_e

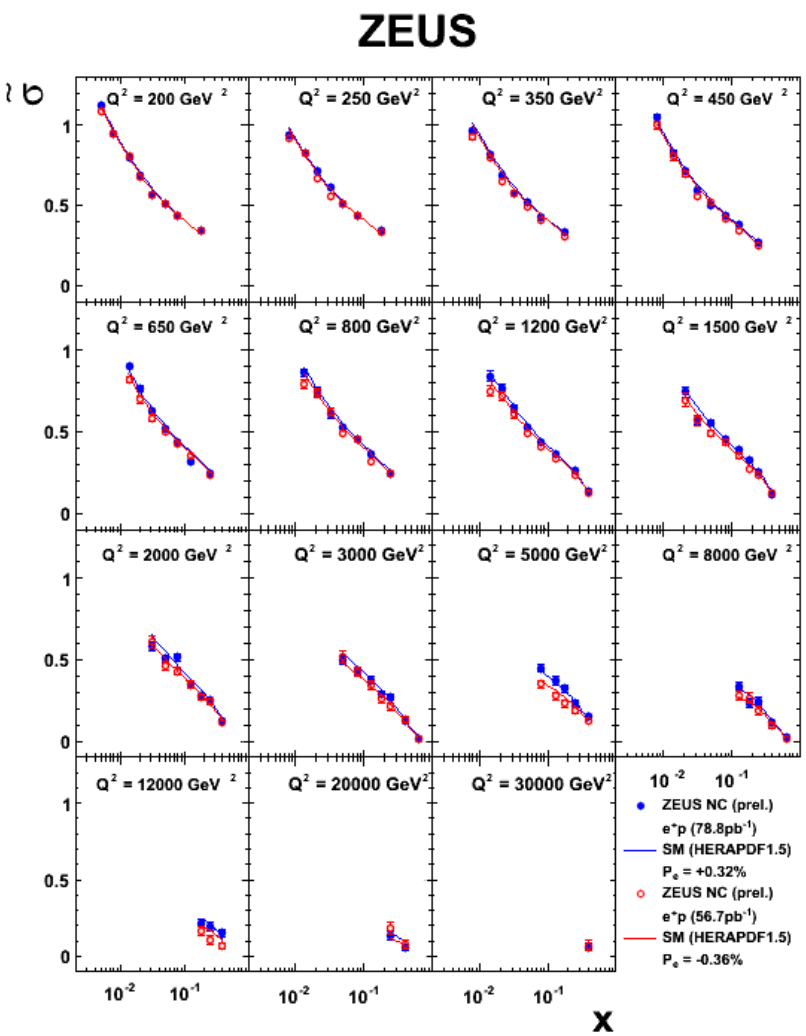

- Closed circles $\rightarrow$ positive P_e.
- Open circles $\rightarrow$ negative P_e.
- Cross-sections nearly identical at low-Q^2.
- Effect of polarisation visible at high-Q^2.

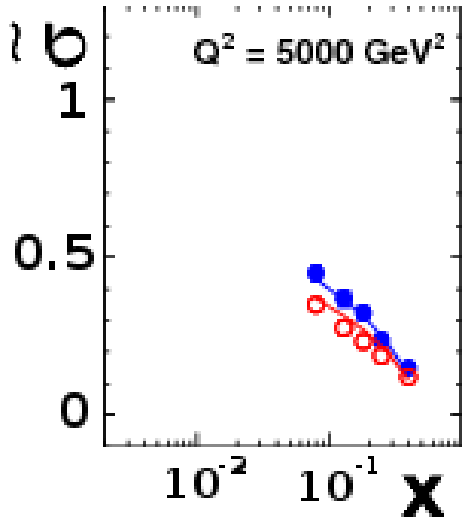

$\tilde{\sigma}$ with $P_e = 0$

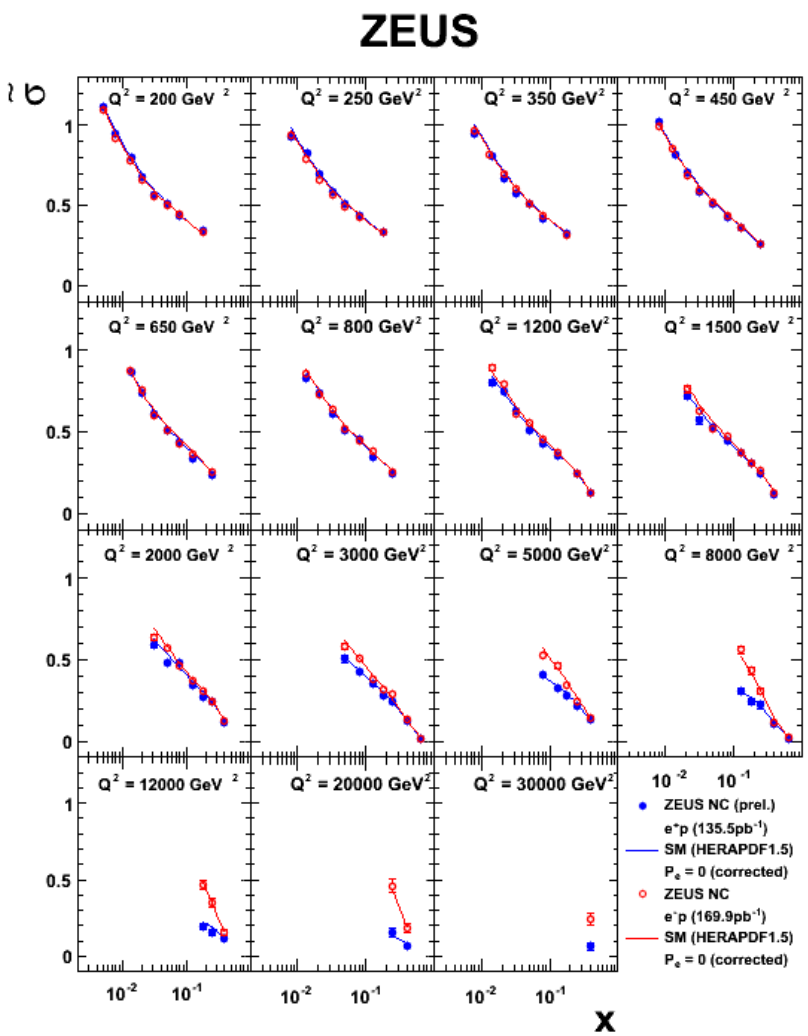

- Closed circles → Full e^+p data set.
- Open circles → Previously measured unpolarised e^-p $\tilde{\sigma}$.
- Difference between e^+p and e^-p clearly seen.
  - SM predictions describe data well.

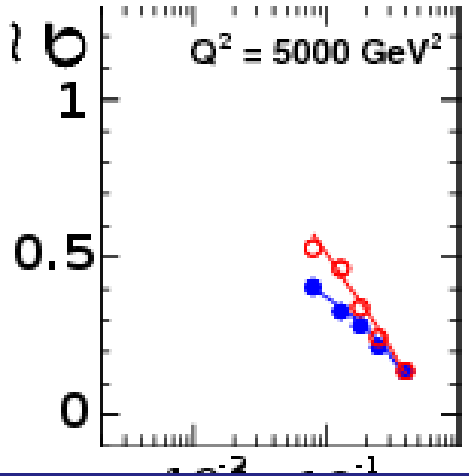

$x\tilde{F}_3$ Extraction (1)

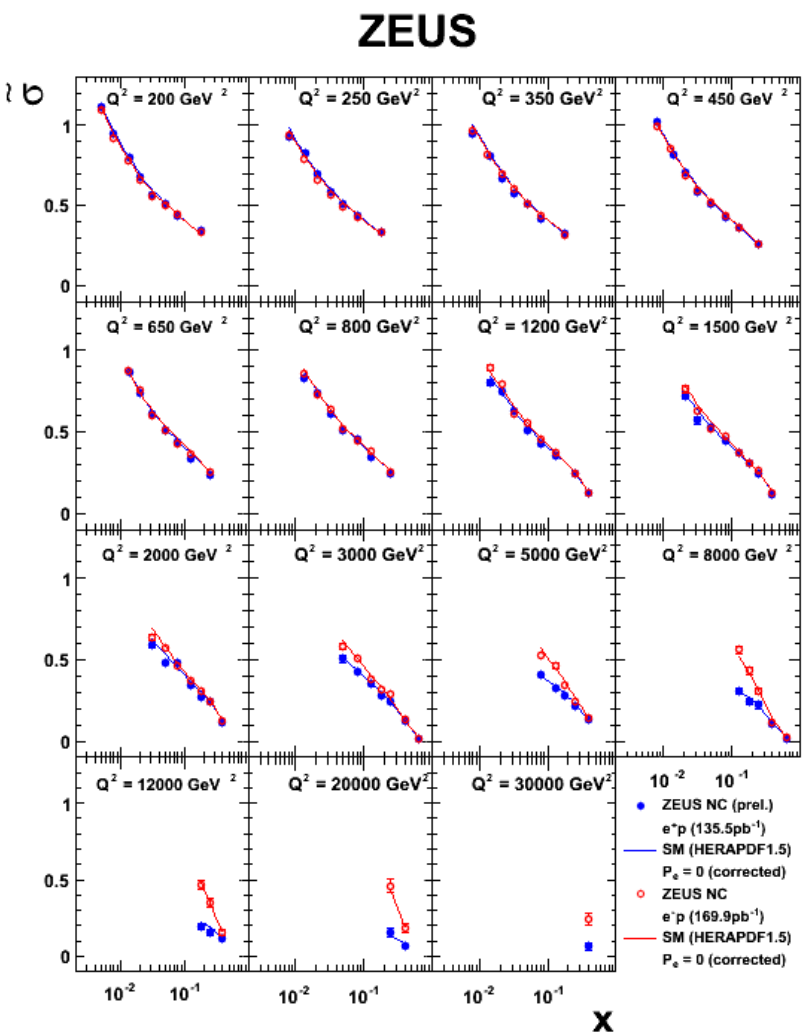

- Difference between e^+p and e^-p gives xF_3:

$$\tilde{\sigma}^{e^-p} - \tilde{\sigma}^{e^+p} = \frac{Y_-}{Y_+} 2x\tilde{F}_3$$

- Expected to contribute at high-Q^2.
- 135.5 pb^{-1} e^+ data, and 169.9 pb^{-1} e^-p data.

$x\tilde{F}_3$ Extraction (2)

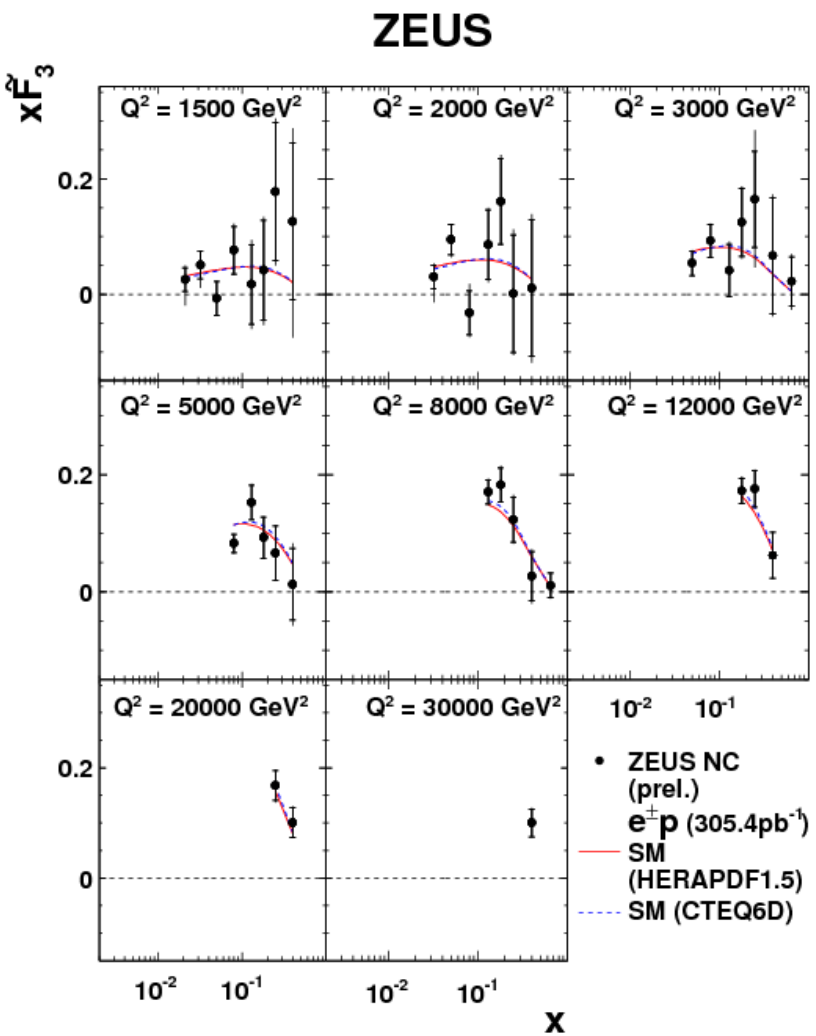

- Difference between e^+p and e^-p gives xF_3:

$$\tilde{\sigma}^{e^-p} - \tilde{\sigma}^{e^+p} = \frac{Y_-}{Y_+} 2x\tilde{F}_3$$

- Expected to contribute at high-Q^2.
- 135.5 pb^{-1} e^+ data, and 169.9 pb^{-1} e^-p data.
  - Most precise $x\tilde{F}_3$ measurement with ZEUS.

$x\tilde{F}_3$ Extraction (2)

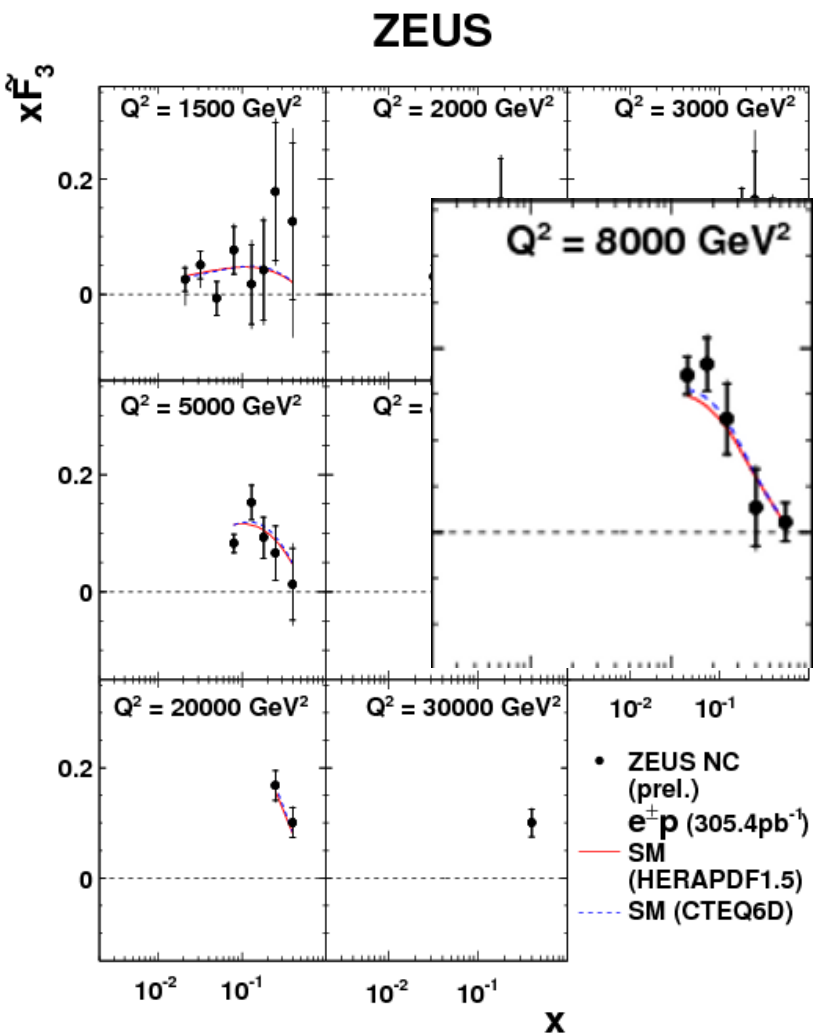

- Difference between e^+p and e^-p gives xF_3:

$$\tilde{\sigma}^{e^-p} - \tilde{\sigma}^{e^+p} = \frac{Y_-}{Y_+} 2x\tilde{F}_3$$

- Expected to contribute at high-Q^2.
- 135.5 pb^{-1} e^+ data, and 169.9 pb^{-1} e^-p data.
  - Most precise $x\tilde{F}_3$ measurement with ZEUS.

High-x:Motivation

- The proton PDFs are poorly constrained at high-x.
  - Variations between PDF sets larger than uncertainty estimates.
- Large x physics is relevant to understanding physics at the LHC.
  - eg. for high mass searches at the LHC.

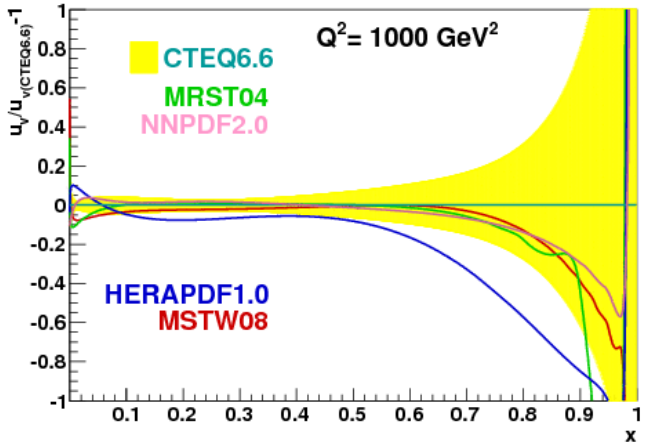

- Can we make a measurement to constrain the PDF uncertainty at high-x?
  - HERA measurements can cover the high-x region up to $x = 1$.

Event Topology

Event with a jet

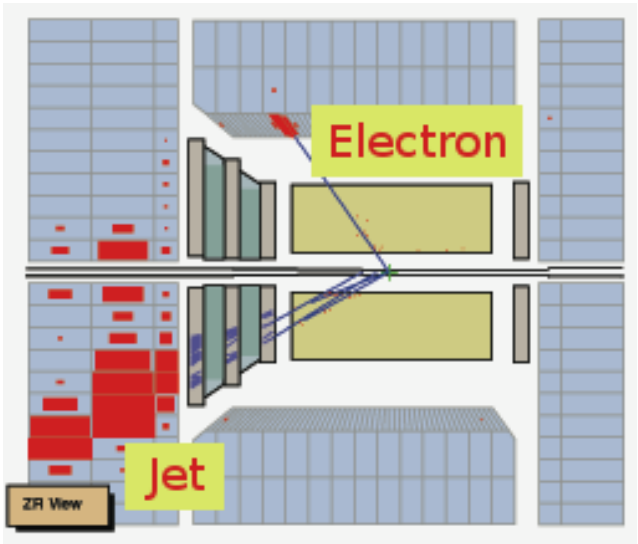

- Jet Definition: $E_T > 10$ GeV, $\theta_{Jet} > 0.11$.
- x reconstructed from jet information.
  - $x < x_{limit}$

Events without a jet

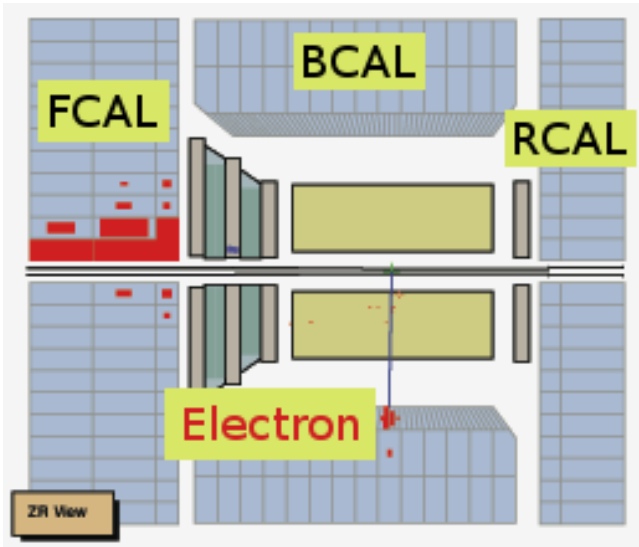

- No Jet information available for reconstruction.
  - Cannot measure $x > x_{limit}$, but we know $x_{limit} < x < 1$.
  - Constrain high-x by using integrated cross-section.

High-x NC e^+p cross-section $d^2\sigma/dxdQ^2$

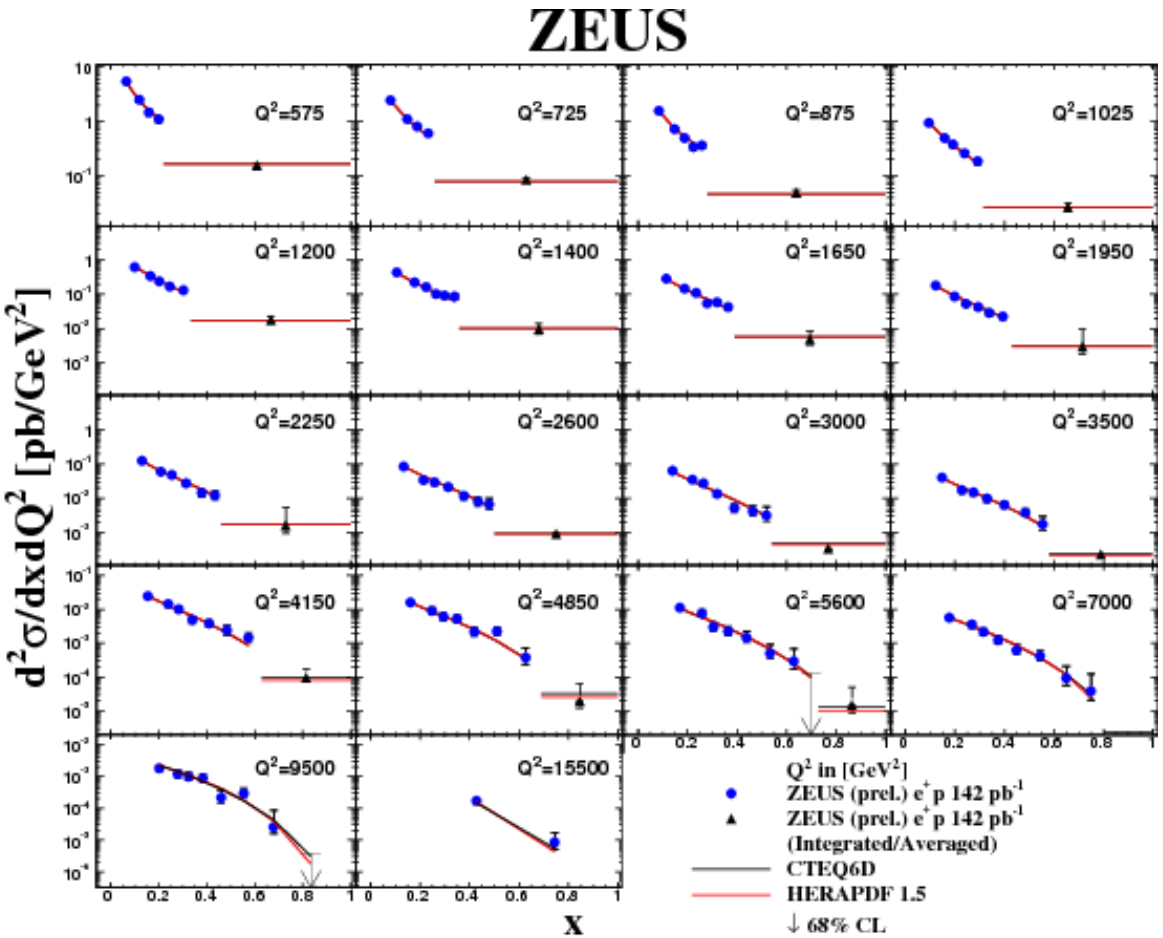

HERAPDF1.5 and **CTEQ6D** (see next slide).

- Circles: points reconstructed using jets.
- Triangles: high-x integrated point.

High-x NC e^+p cross-section $d^2\sigma/dxdQ^2$: Comparison to HERAPDF1.5

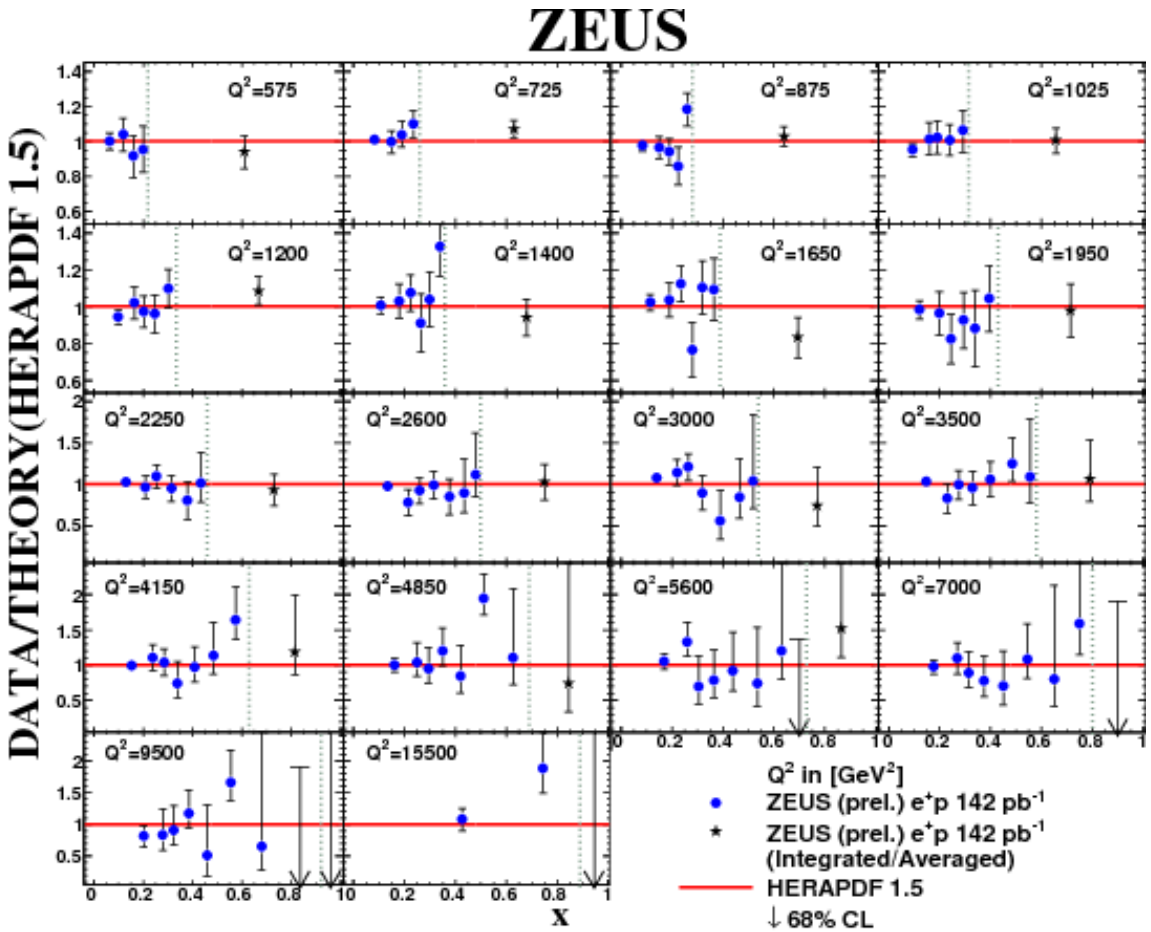

SM expectation in good agreement with data

High-x NC e^+p cross-section $\tilde{\sigma}$: Comparison to e^-p

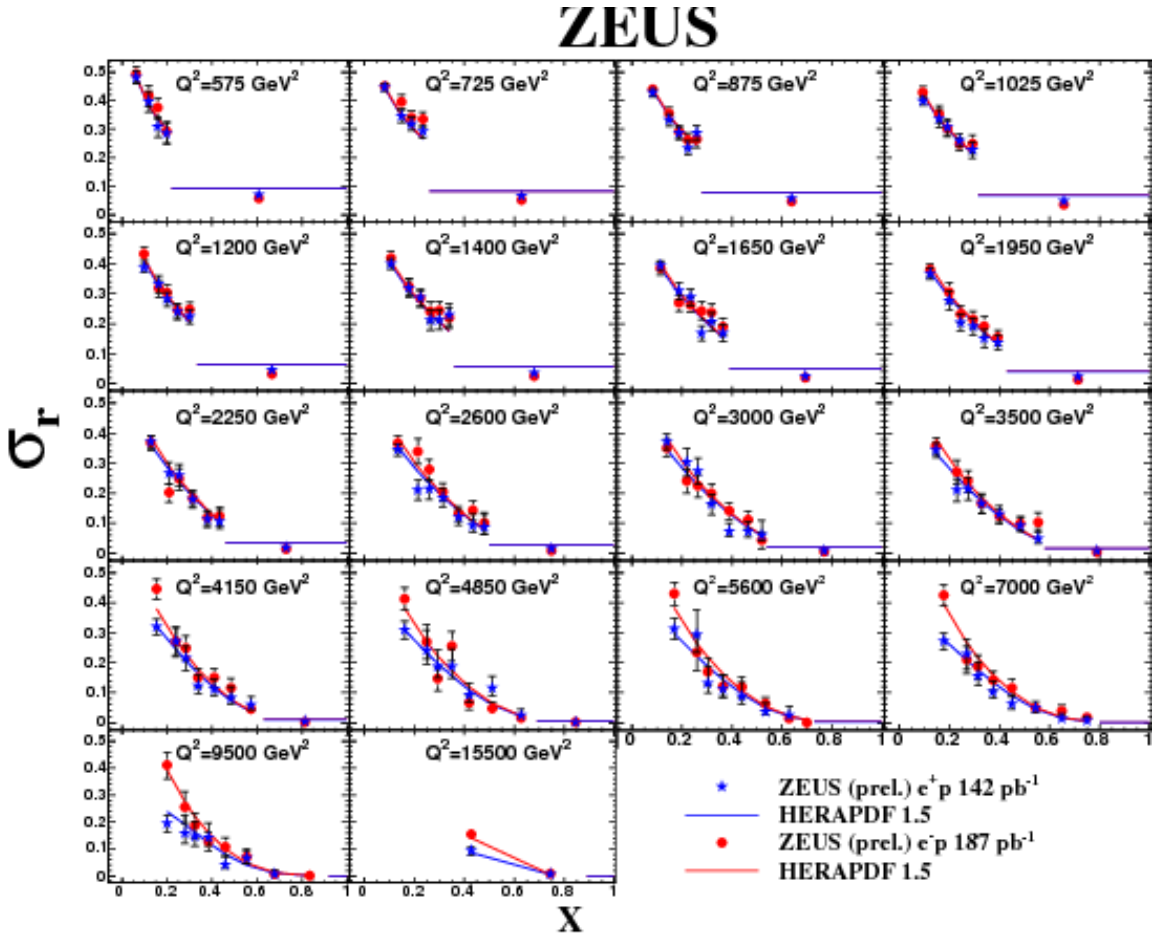

- Stars → Full e^+p data set.
- Circles → Previously measured e^-p σ_R.
- Difference between e^+p and e^-p clearly seen.
  - Described well by SM predictions.

Summary

- The ZEUS HERA-II inclusive results are almost finished (preliminary NC results shown here).
  - e^+p CC results have already been published.
  - e^+p NC is almost finished.
  - Final high-x e^+p NC results shown, completing the high-x HERA-II analyses.
- EW theory tested in both inclusive CC and NC results.
  - Polarised CC and NC single and reduced cross-sections.
  - $x\tilde{F}_3$ extraction.
- Results will help constrain the HERAPDF (CC results have already been included).
  - Unpolarised CC and NC single and reduced cross-sections.
  - High-x NC analysis will better constrain the PDFs at high-x.

Charged Current Sample (e^+p Data)

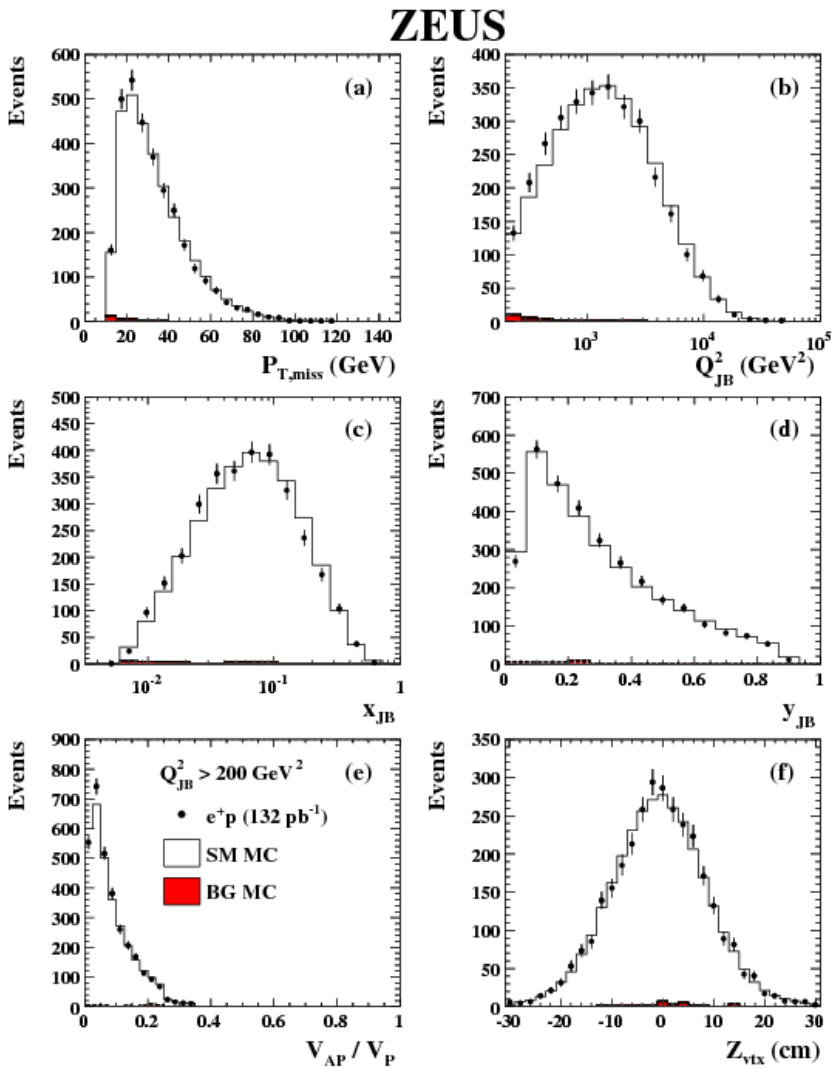

- Results published in 2010.
  - Eur. Phys. J. C (2010) 70: 945963.
- e^+p data, taken 2006-07, $\mathcal{L} = 132pb^{-1}$
  - $P_e = +33\%$, $\mathcal{L} = 75.8pb^{-1}$
  - $P_e = -36\%$, $\mathcal{L} = 56.0pb^{-1}$
- Linear dependence of the cross-section on P_e.
- Data well understood.

Neutral Current Sample (e^+p Data)

- New result (ZEUS-prel-11-003).
  - Missing result of the HERA-II ZEUS high-Q^2 inclusive analyses.

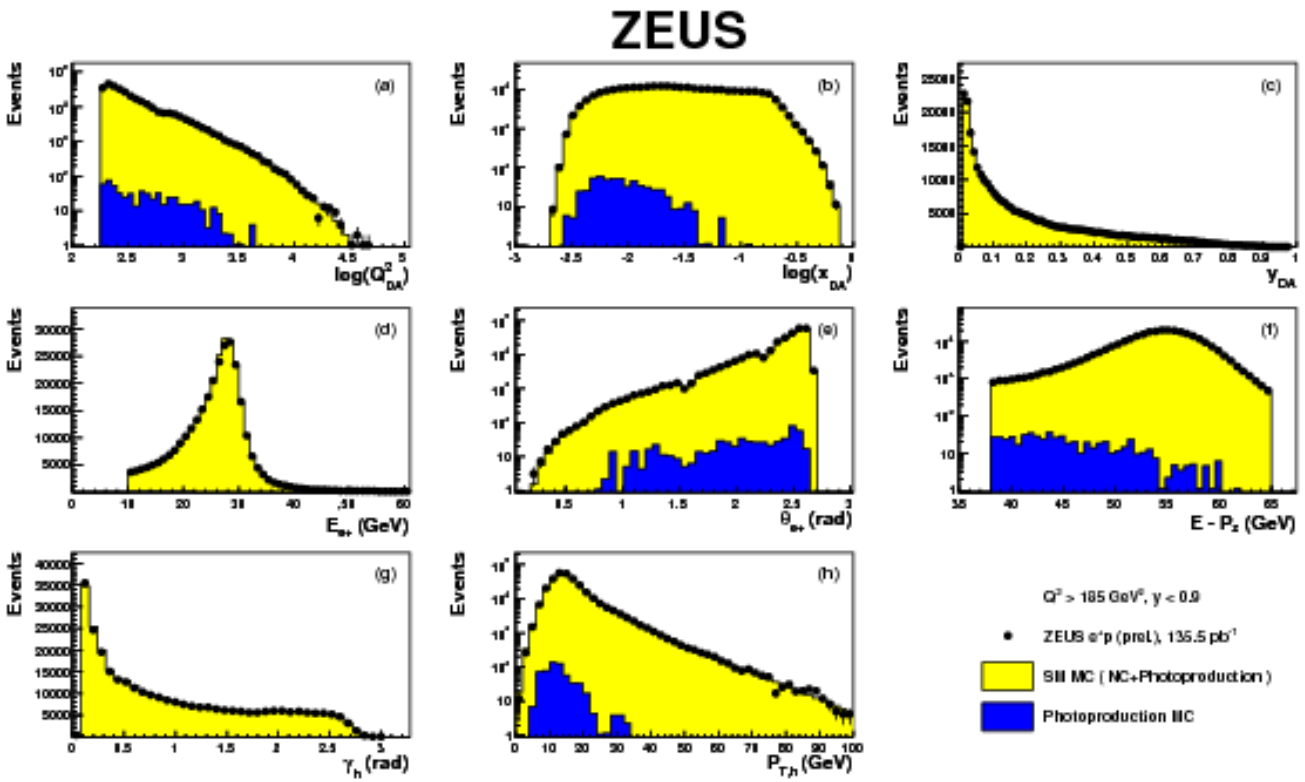

- e^+p data, taken 2006-07, $\mathcal{L} = 135 pb^{-1}$
  - $P_e = +32\%$, $\mathcal{L} = 78.8 pb^{-1}$
  - $P_e = -36\%$, $\mathcal{L} = 56.7 pb^{-1}$
- Kinematic range: $Q^2 > 185 GeV$ and $y < 0.9$.
- Data well described.

Control Plots

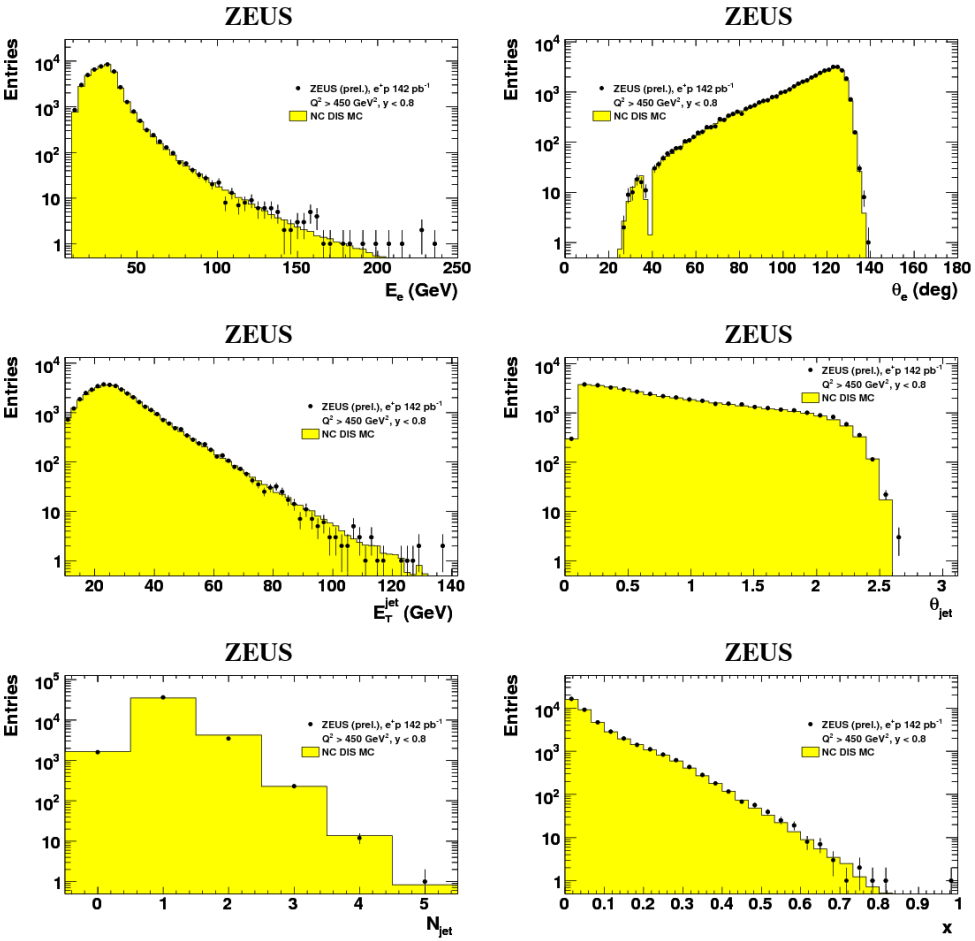

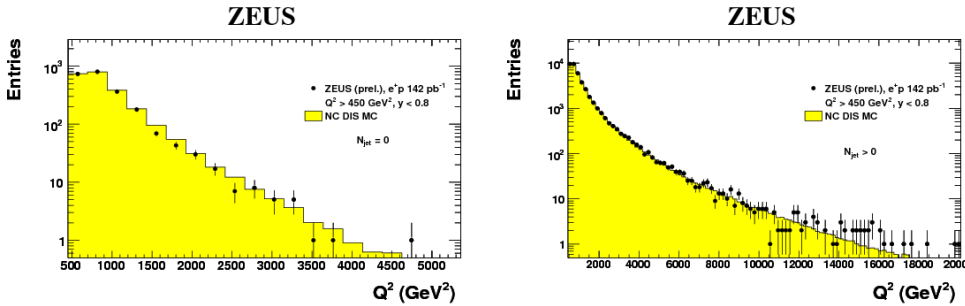

- New result (ZEUS-prel-11-004).
- e^+p data, taken 2006-07, $\mathcal{L} = 143pb^{-1}$
- Electron and Jet variables well described by MC.
- Kinematic variables well described for events with $N_{Jet} = 0$ and $N_{Jet} > 0$.